

National Aeronautics and Space Administration

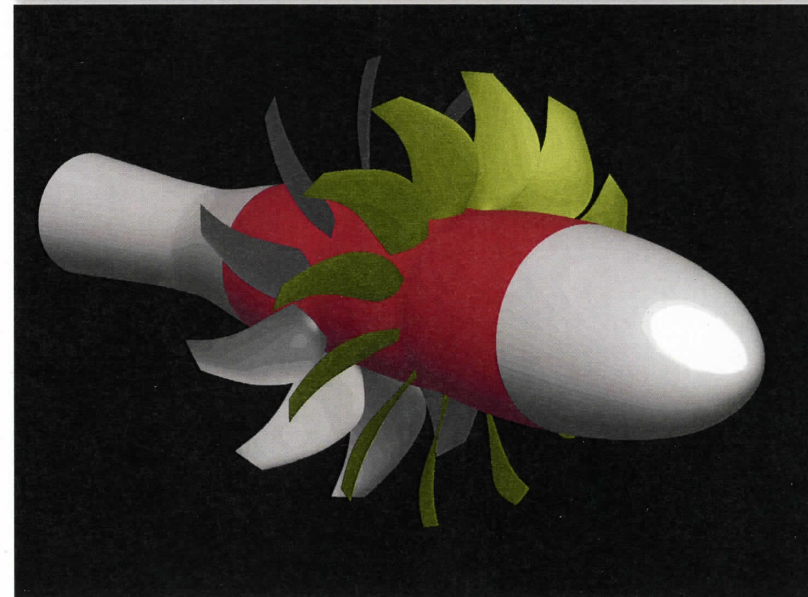


# Prediction of Tone Noise from Open Rotors

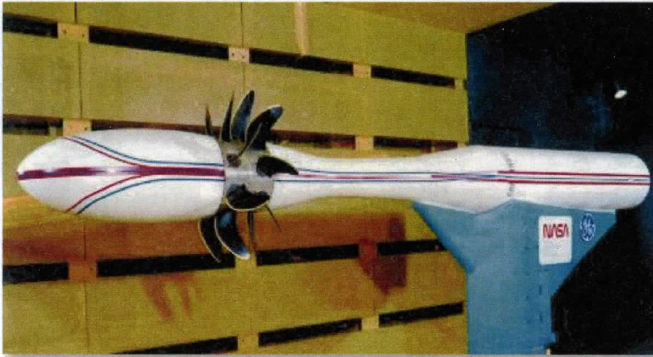
**Ed Envia**  
NASA Glenn Research Center

OSU  
January 30, 2012

This work has been supported by  
the Subsonic Fixed Wing (SFW) and  
Environmentally Responsible Aviation (ERA) Projects.



# Why Open Rotors?



Un-ducted Fan (UDF) Model in  
NASA Wind Tunnel (1985)



GE UDF Engine  
on MD-80 Aircraft (1987)



PW/Allison 578-DX Engine  
on MD-80 Aircraft (1989)

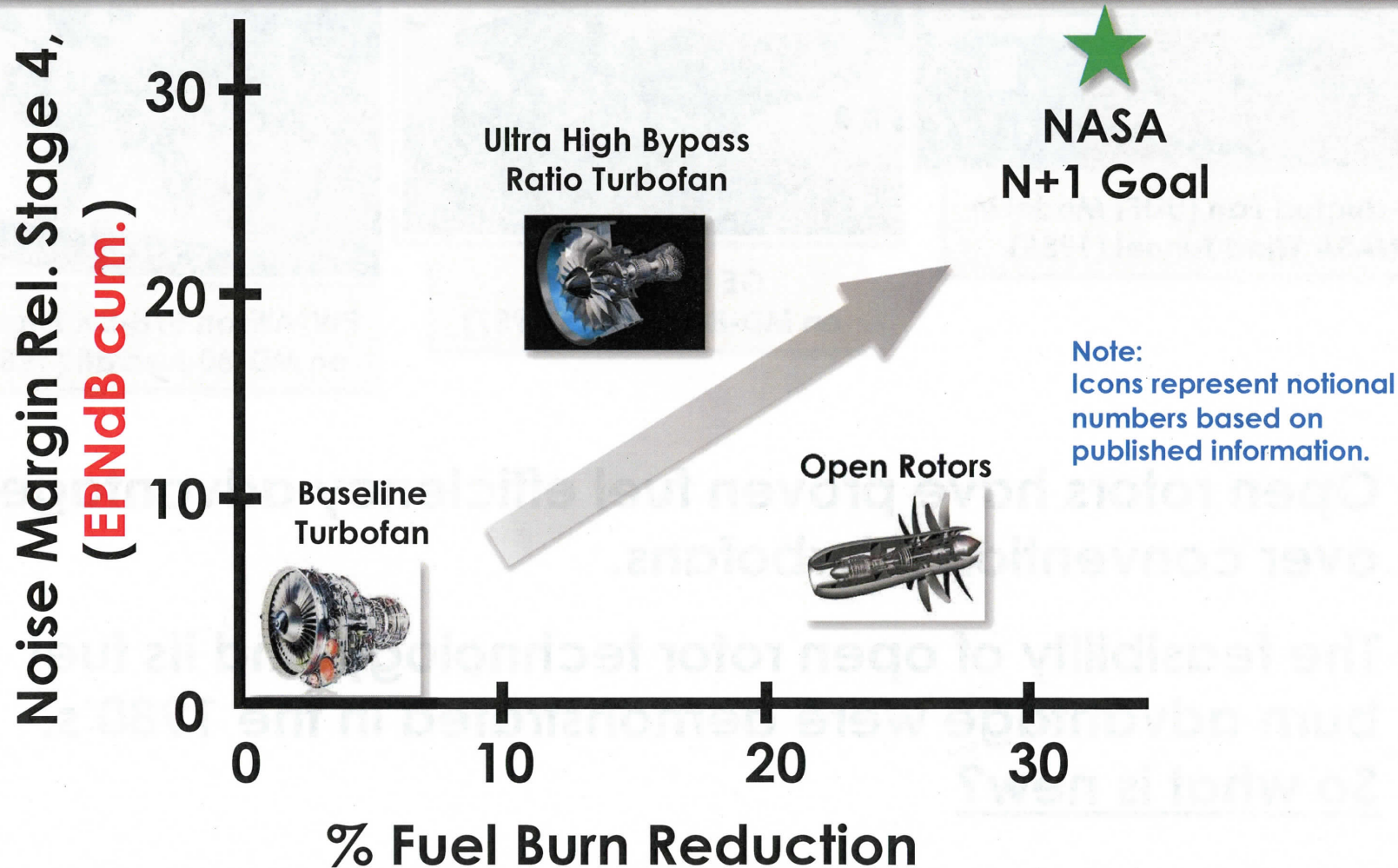
- ❖ Open rotors have proven fuel efficiency advantage over conventional turbofans.
- ❖ The feasibility of open rotor technology and its fuel burn advantage were demonstrated in the 1980's.  
So what is new?



# Modern Open Rotors



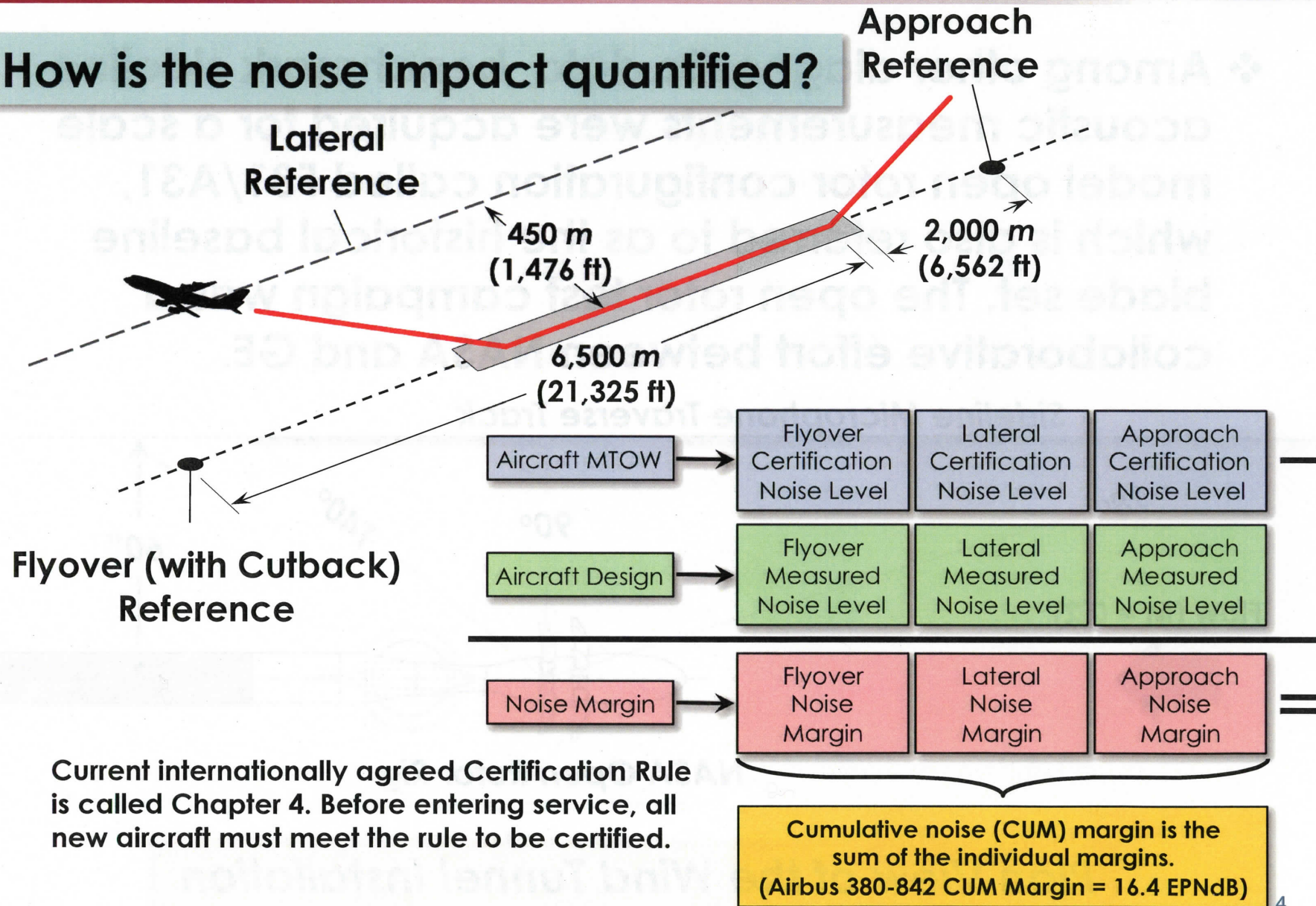
Advances in 3D aerodynamic design tools have made possible open rotor systems that can meet the current noise rules while maintaining their fuel burn advantage. The goal is to make them acoustically competitive with the next generation turbofans.



# Noise Metric: Cumulative EPNdB



How is the noise impact quantified?

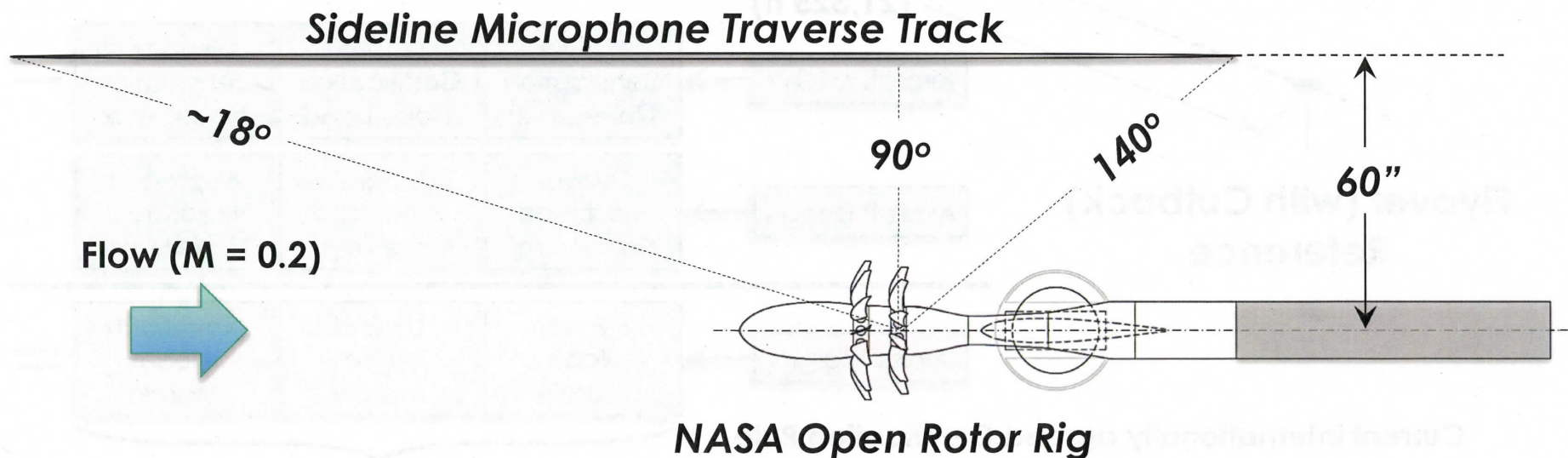




# NASA Open Rotor Wind Tunnel Test



- ❖ Among other diagnostic data, benchmark sideline acoustic measurements were acquired for a scale model open rotor configuration called F31/A31, which is also referred to as the historical baseline blade set. The open rotor test campaign was a collaborative effort between NASA and GE.

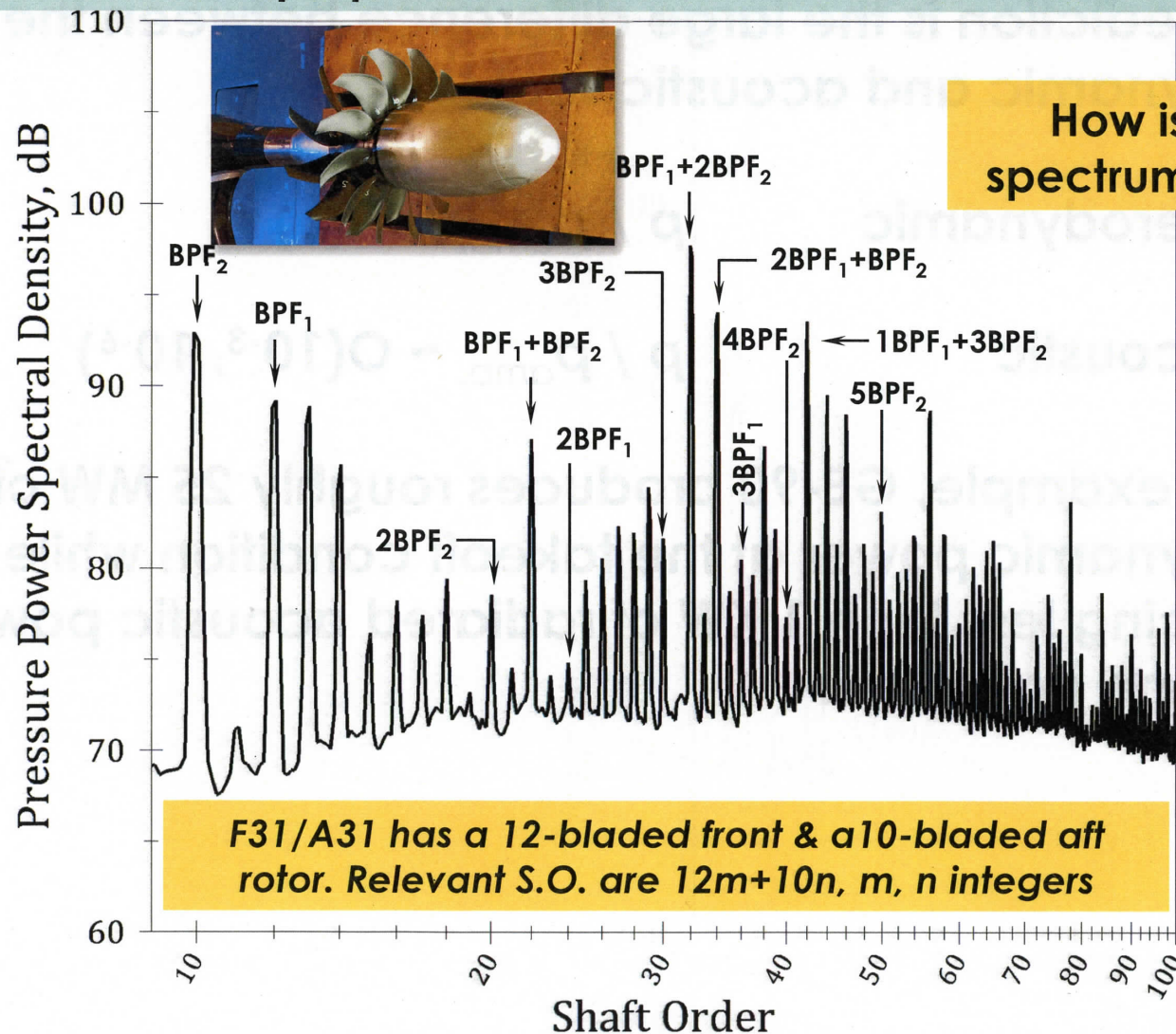


**Plan View of the Wind Tunnel Installation**

# Open Rotor Noise Spectrum



Measured F31/A31 Sideline Narrowband Acoustic Spectrum at 90° Angle  
Open rotors have a preponderance of tones in their acoustic spectra.





# Modeling Challenge



- ❖ The fundamental challenge of aeroacoustic modeling and prediction is the large difference between the aerodynamic and acoustic scales:

Aerodynamic  $p / p_{amb.} \sim O(1)$

Acoustic  $p / p_{amb.} \sim O(10^{-3}, 10^{-6})$

- ❖ As an example, GE-90 produces roughly 25 MW of aerodynamic power at the takeoff condition while producing less than 1 KW of radiated acoustic power at the same condition.

# Modeling Strategy

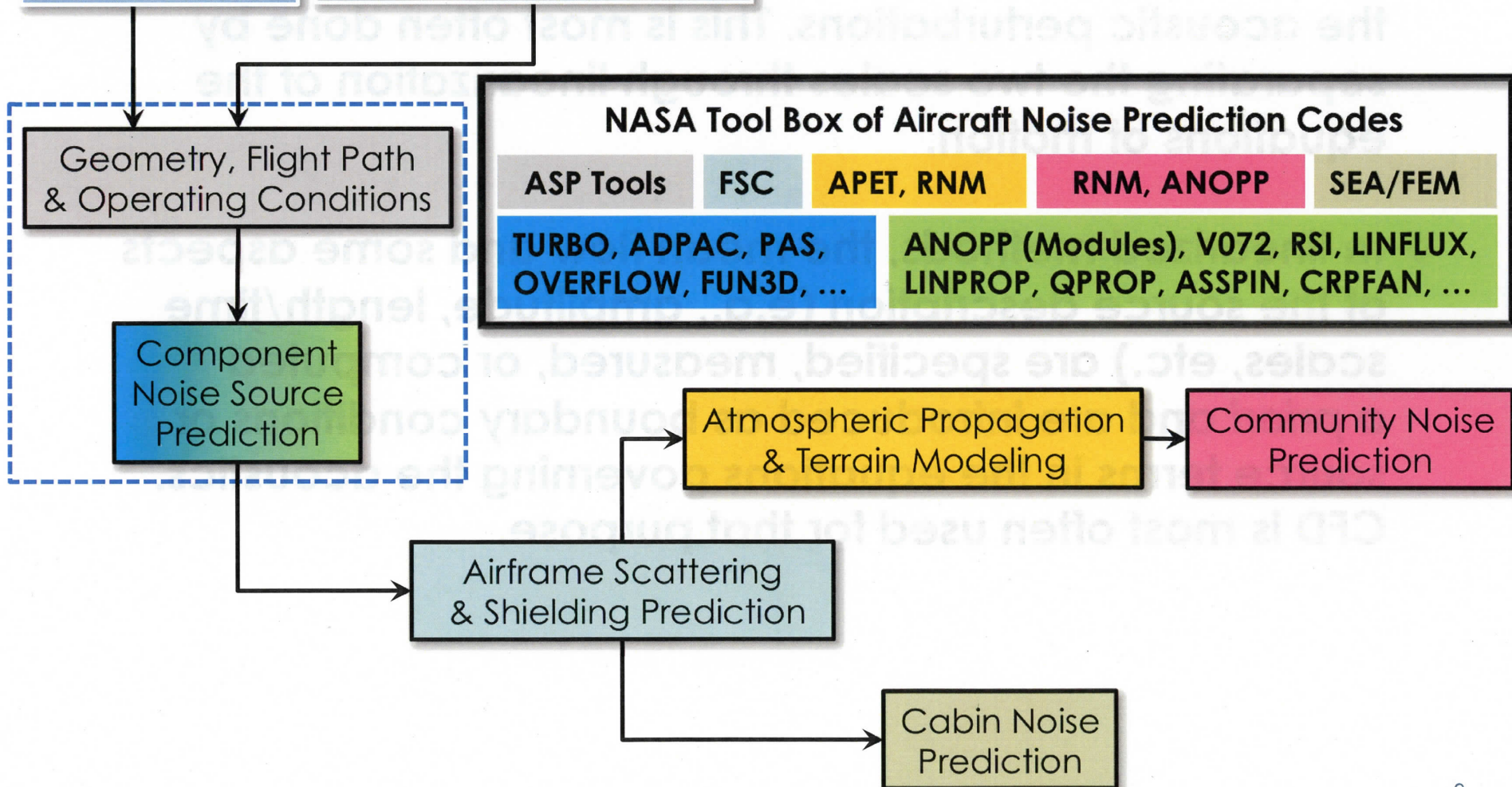
---



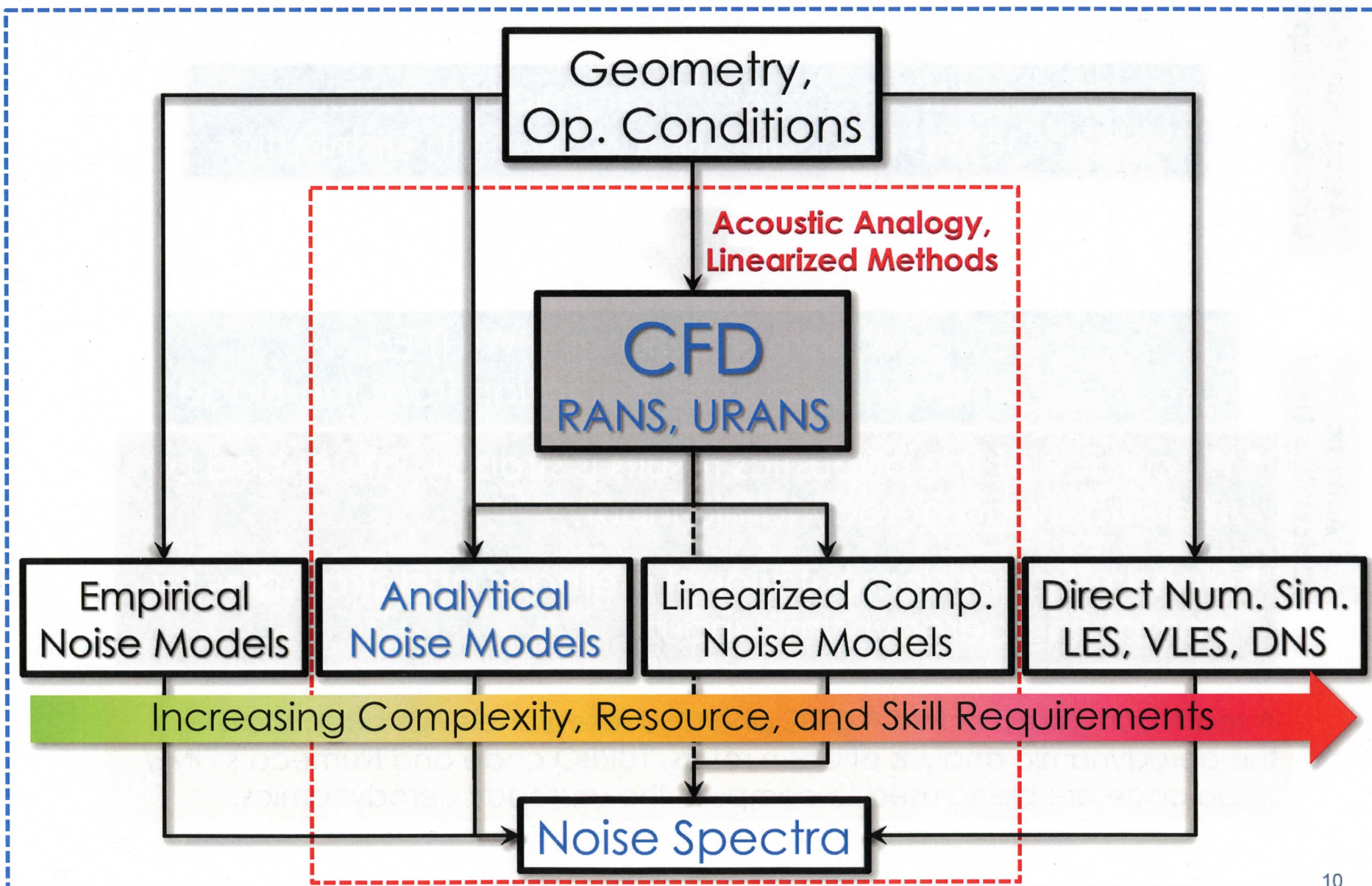
- ❖ This difference necessitates the development of specialized modeling techniques to adequately resolve the acoustic perturbations. This is most often done by separating the two scales through linearization of the equations of motion.
- ❖ In linearized methods, the mean flow and some aspects of the source description (e.g., amplitude, length/time scales, etc.) are specified, measured, or computed *a priori* and are introduced as boundary conditions or source terms in the equations governing the acoustics. CFD is most often used for that purpose.



# Acoustic Prediction Framework



# Component Noise Source Prediction





# Acoustic Analogy



Aerodynamic  
Calculation Step

Steady/Unsteady Aerodynamic Simulations  
Used to Define Acoustic Source Strength Distribution



Acoustic  
Calculation Step

Ffowcs-Williams Hawkins (FW-H) Eq.  
Used for Computing Acoustic Radiation from the Blade

- Accuracy of the acoustics results is strongly influenced by the underlying aerodynamic input.
- Need efficient computational methods and strategies for computing aerodynamic input.

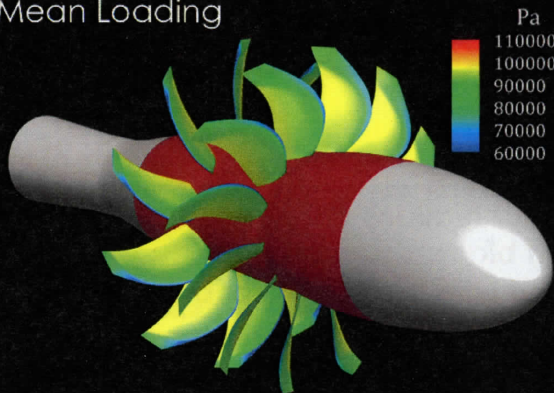
A team comprised of NASA GRC and OSU researchers has been tackling the aerodynamic analysis of open rotors. TURBO code and Numeca's FINE/Turbo code are being used to compute the unsteady aerodynamics.



# Aerodynamic Input

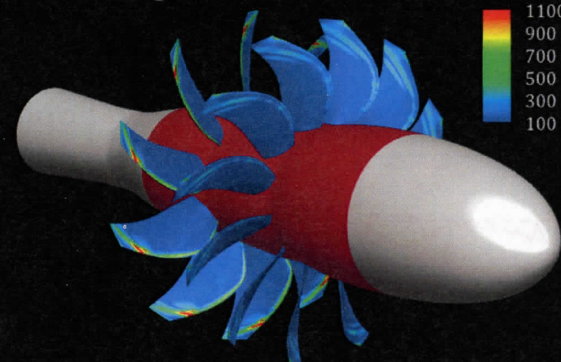


Mean Loading

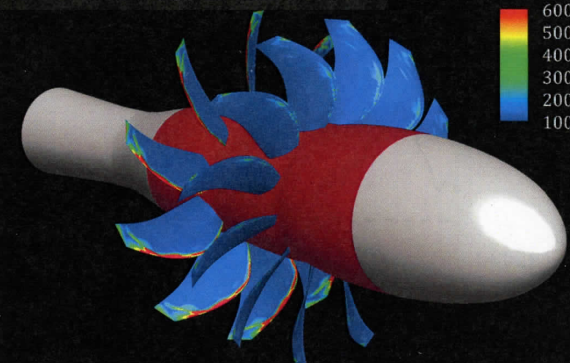


Ex.: TURBO Unsteady RANS Simulation of F31/A31 at Nominal Takeoff Condition (Corrected RPMs = 6,625)

1<sup>st</sup> Loading Harmonic



2<sup>nd</sup> Loading Harmonic



12-Bladed Front Rotor 10-Bladed Aft Rotor		Measured	Predicted
Thrust (lbf)	Front Rotor	303	304
	Aft Rotor	305	309
Torque (ft-lb)	Front Rotor	178	182
	Aft Rotor	171	177
Power (hp)	Front Rotor	225	230
	Aft Rotor	216	223

Contour plots and integrated quantities shown here were computed from a simulation carried out at OSU by Trevor Goerig.

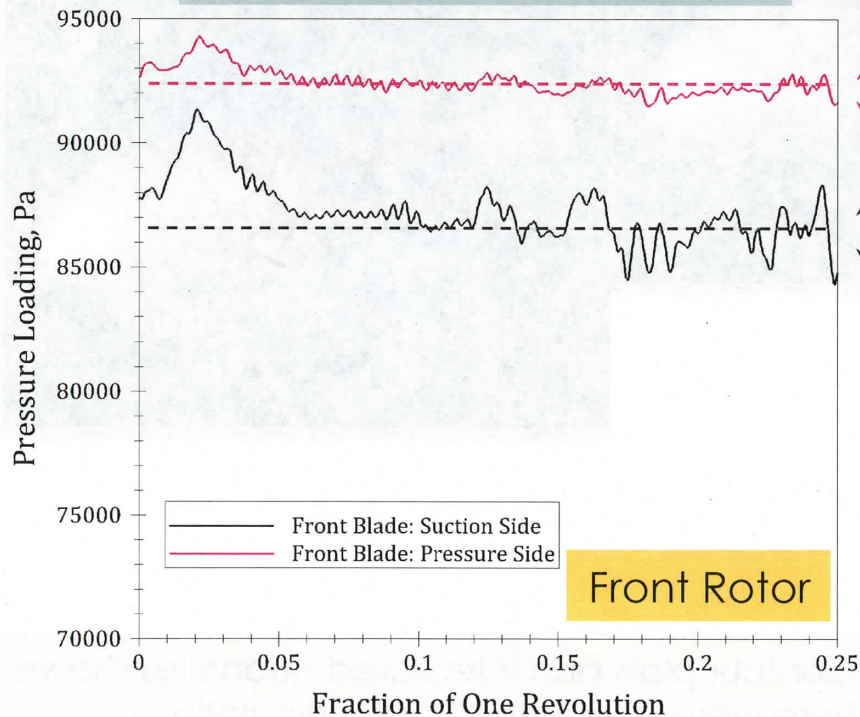


# Aerodynamic Input (Cont'd)

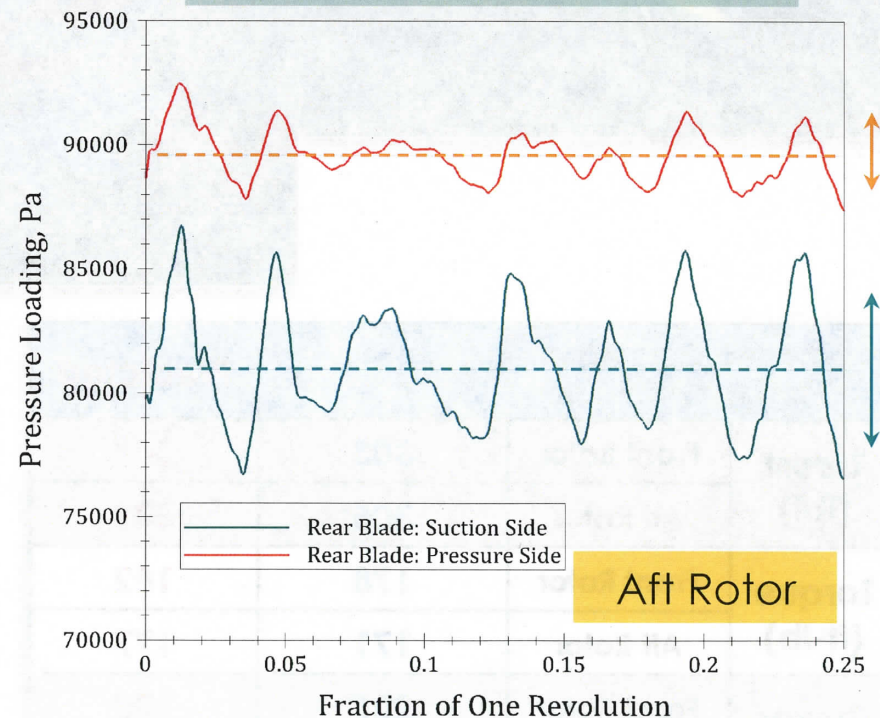


## ❖ Aerodynamic Calculation — Time Histories

Overall loading is higher on the front blade's pressure side, but fluctuating loading is larger on its suction side.



Loading fluctuations are even larger on the aft blade's suction side compared with the front rotor blade.

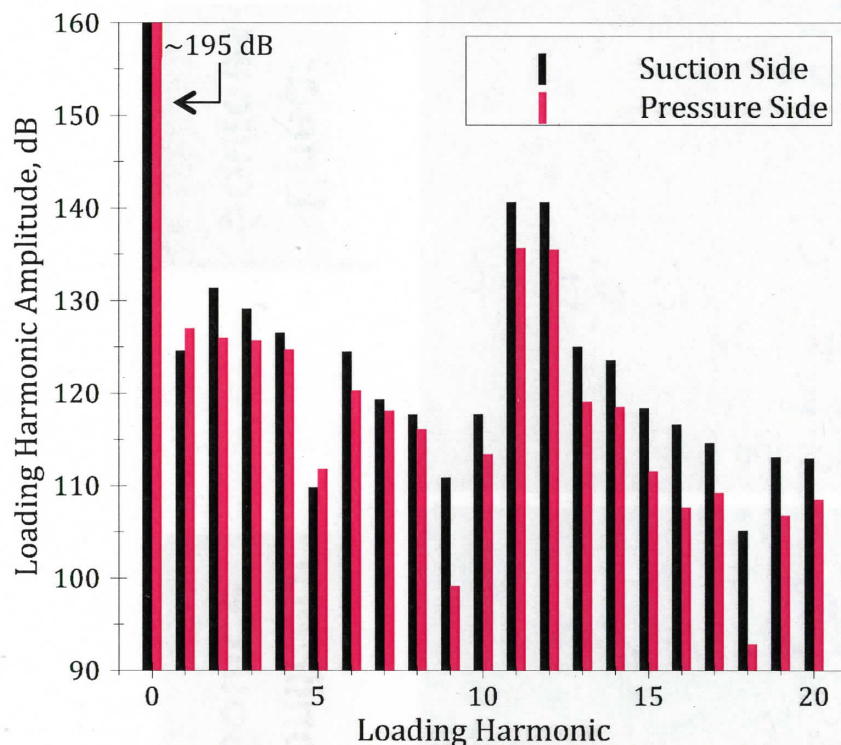


# Computed Blade Loading Spectra

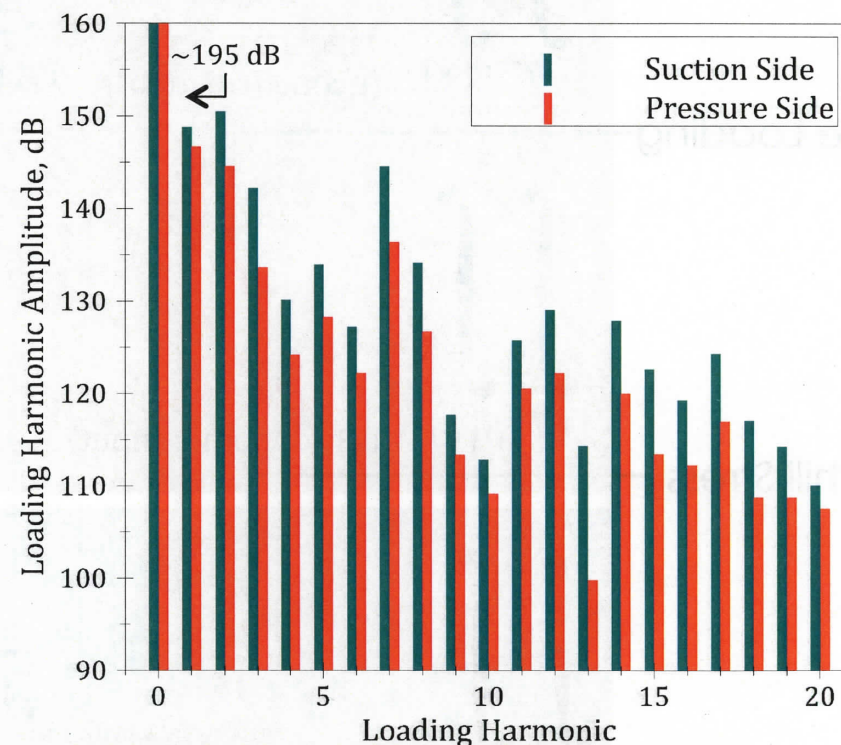


There are significant differences between the unsteady loading content of the two rotors. Expect to see differences in the relative acoustic contributions of the front and aft blade rows.

Front Blade



Rear Blade



There is several orders of magnitude difference between the mean and the unsteady components. Yet, wind tunnel data indicate that the unsteady loading component can contribute significantly to the overall noise of an open rotor.



# Acoustic Solution – FW-H Equation



Blade Normal Velocity

$$p(\vec{x}, t) = \int_{-T}^T \int_{S(\tau)} \underbrace{\rho_0 v_n}_{\text{Thickness Source (geometric input)}} \underbrace{\frac{D_0 G}{D\tau}}_{\text{Propagation}} ds d\tau +$$

Green's Function

Blade Loading

$$\int_{-T}^T \int_{S(\tau)} \underbrace{F_j}_{\text{Loading Source (aerodynamic input)}} \underbrace{\frac{\partial G}{\partial y_j}}_{\text{Propagation}} ds d\tau +$$

Lighthill Stress

$$\int_{-T}^T \int_{V(\tau)} \underbrace{T_{jk}}_{\text{Quadrupole Source (aerodynamic input)}} \underbrace{\frac{\partial^2 G}{\partial y_j \partial y_k}}_{\text{Propagation}} ds d\tau$$

Linear  
Sources

Nonlinear  
Source



# Freq.-Domain Representation: Single Rotor

$T$ : Thickness Noise  
 $L$ : Loading Noise  
 $Q$ : Quadrupole Noise

## Large Blade Count Asymptotic Approximation to the FW-H Eq.

(Ref.: E. Envia, AIAA Journal, Vo. 32, No. 2, February 1994)

$$p(\vec{x}, t) = \sum_{m=-\infty}^{\infty} \underbrace{\left( p_{mB}^{(T)}(\vec{x}) + p_{mB}^{(L)}(\vec{x}) + p_{mB}^{(Q)}(\vec{x}) \right)}_{\text{Tone Amplitude}} e^{-i \overbrace{mB\Omega}^{\text{Tone Frequency}} t}$$

$B$  Blade Count  
 $\Omega$  Rotational Speed

$$p_{mB}^{(T,L,Q)}(\vec{x}) = \int_{S_0, V_0} e^{-imB\Psi} \left\{ d_0^{(T,L,Q)} \frac{Ai\left[ (mB)^{2/3} \gamma^2 \right]}{(mB)^{1/3}} + d_1^{(T,L,Q)} \frac{Ai'\left[ (mB)^{2/3} \gamma^2 \right]}{(mB)^{2/3}} \right\} ds$$

Airy Function & Its Derivative

Surface or volume  
 integral computed  
 Using quadrature

Uniform asymptotic representation of the FW-H Eq. This formula is much more efficient than carrying out the  $\tau$  integration numerically when the parameter  $mB$  is large.

The representation is valid across the tip speed regime (subsonic to supersonic) and applicable to any observer position (near- or far-field). The code based on that solution for the thickness & loading sources is called LINPROP and that for the quadrupole source is called QPROP. The Data-theory comparisons for single rotation configurations for both codes can be found in the cited reference.



# Extension to Open Rotors



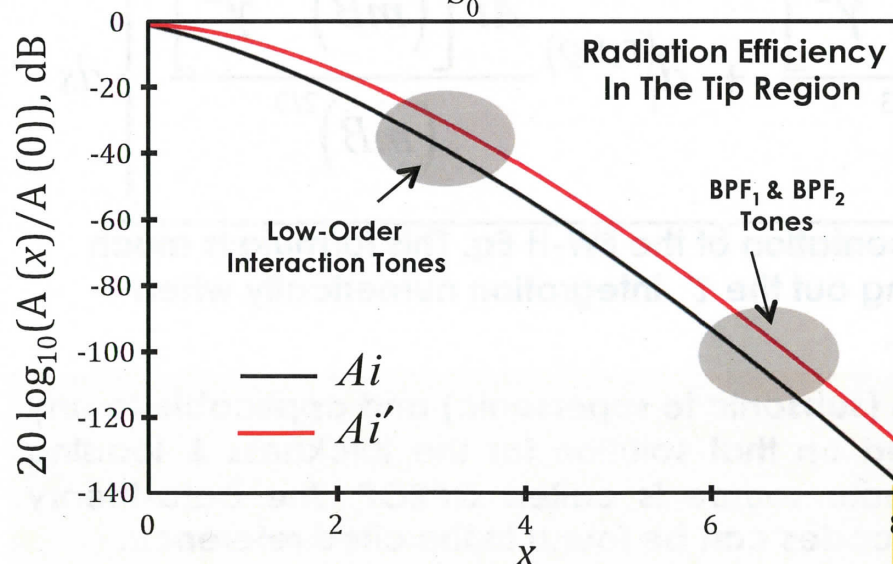
\* Only loading noise term needs to be modified

$$p^{(L)}(\vec{x}, t) = \sum_{m=-\infty}^{\infty} \sum_{k=-\infty}^{\infty} \underbrace{p_{mB_1, kB_2}^{(L)}(\vec{x})}_{\text{Tone Amplitude}} e^{-i \overbrace{(mB_1\Omega_1 + kB_2\Omega_2)t}^{\text{Tone Frequency}}}$$

$m$  is noise harmonic index  
 $k$  is loading harmonic index

Blade counts and rotational speeds need not be the same

$$p_{mB_1, kB_2}^{(L)}(\vec{x}) = \int_{S_0} e^{-i(mB_1 - kB_2)\tilde{\Psi}(\Omega_1, \Omega_2)} \left\{ d_{0,k}^{(L)} \frac{Ai\left[(mB_1 - kB_2)^{2/3} \tilde{\gamma}^2\right]}{(mB_1 - kB_2)^{1/3}} + \right.$$

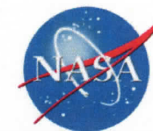


$$d_{1,k}^{(L)} \frac{Ai'\left[(mB_1 - kB_2)^{2/3} \tilde{\gamma}^2\right]}{(mB_1 - kB_2)^{2/3}} \Bigg\} ds$$

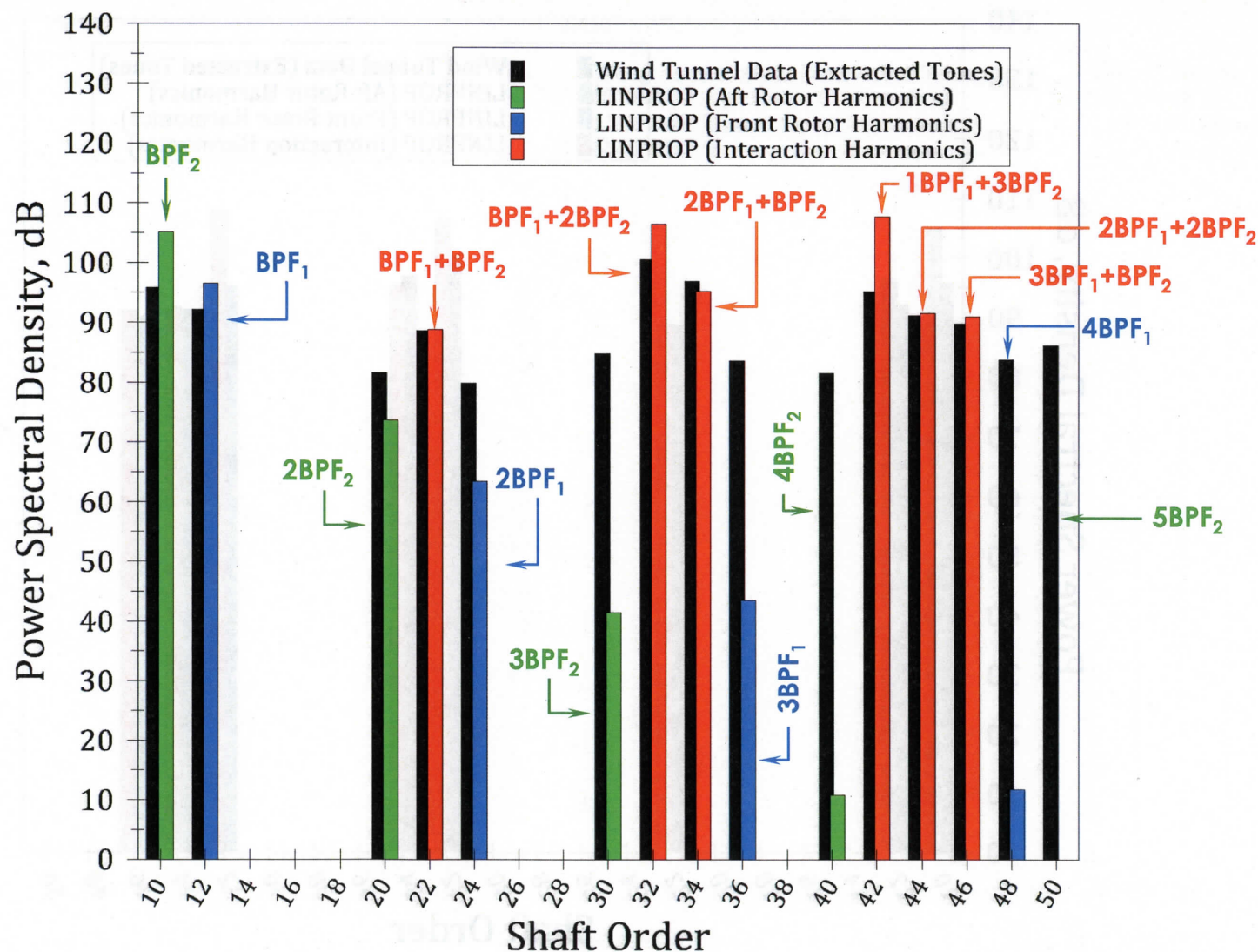
Tone radiation efficiency is effectively controlled by this index parameter

Weaker loading harmonic amplitude of interaction tones compared with the primary rotor tones is compensated for by their much higher radiation efficiency.

# Data-Theory Comparisons



Only thickness and loading sources are considered in this comparison.

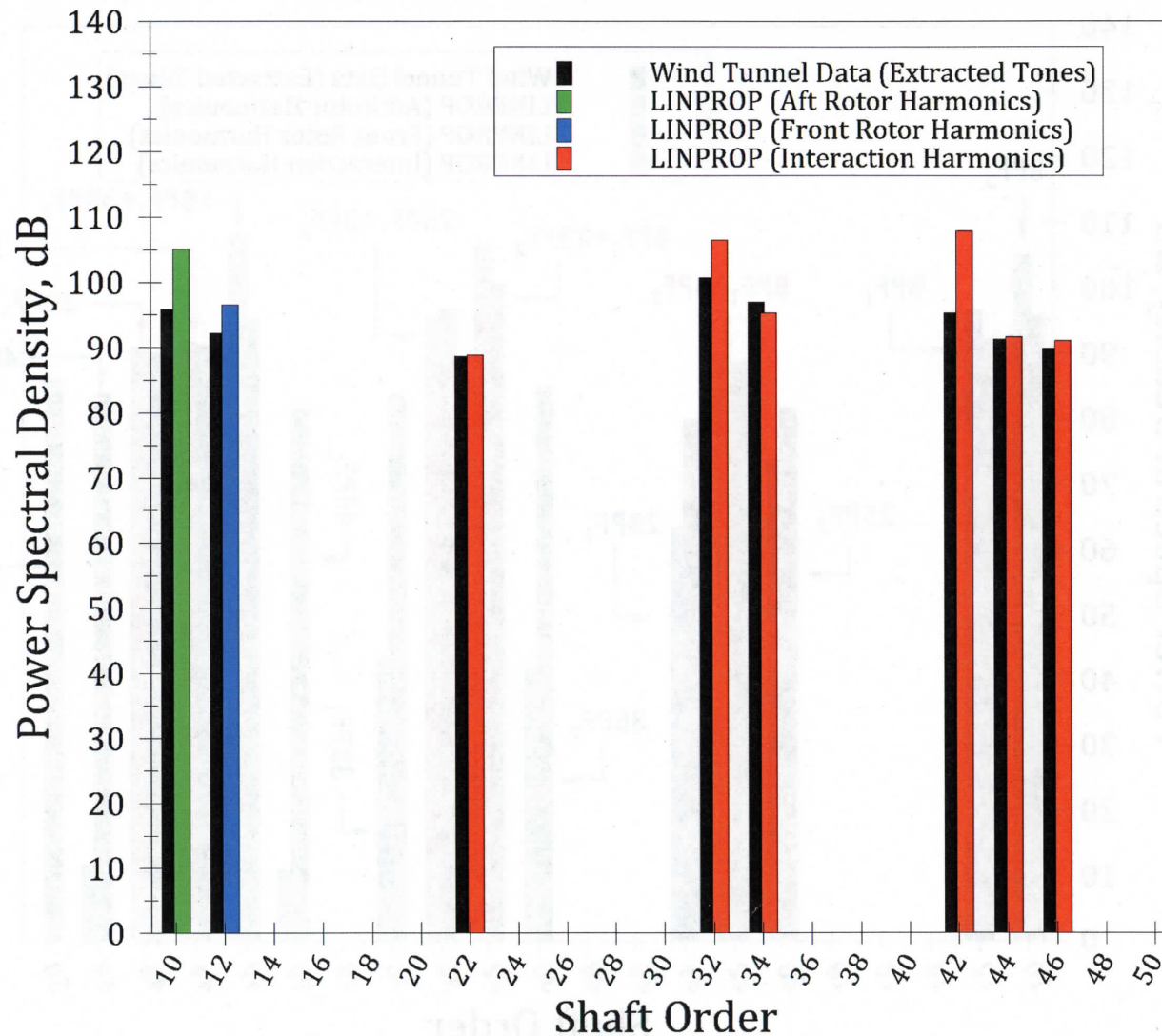




# Data-Theory Comparisons (Cont'd)



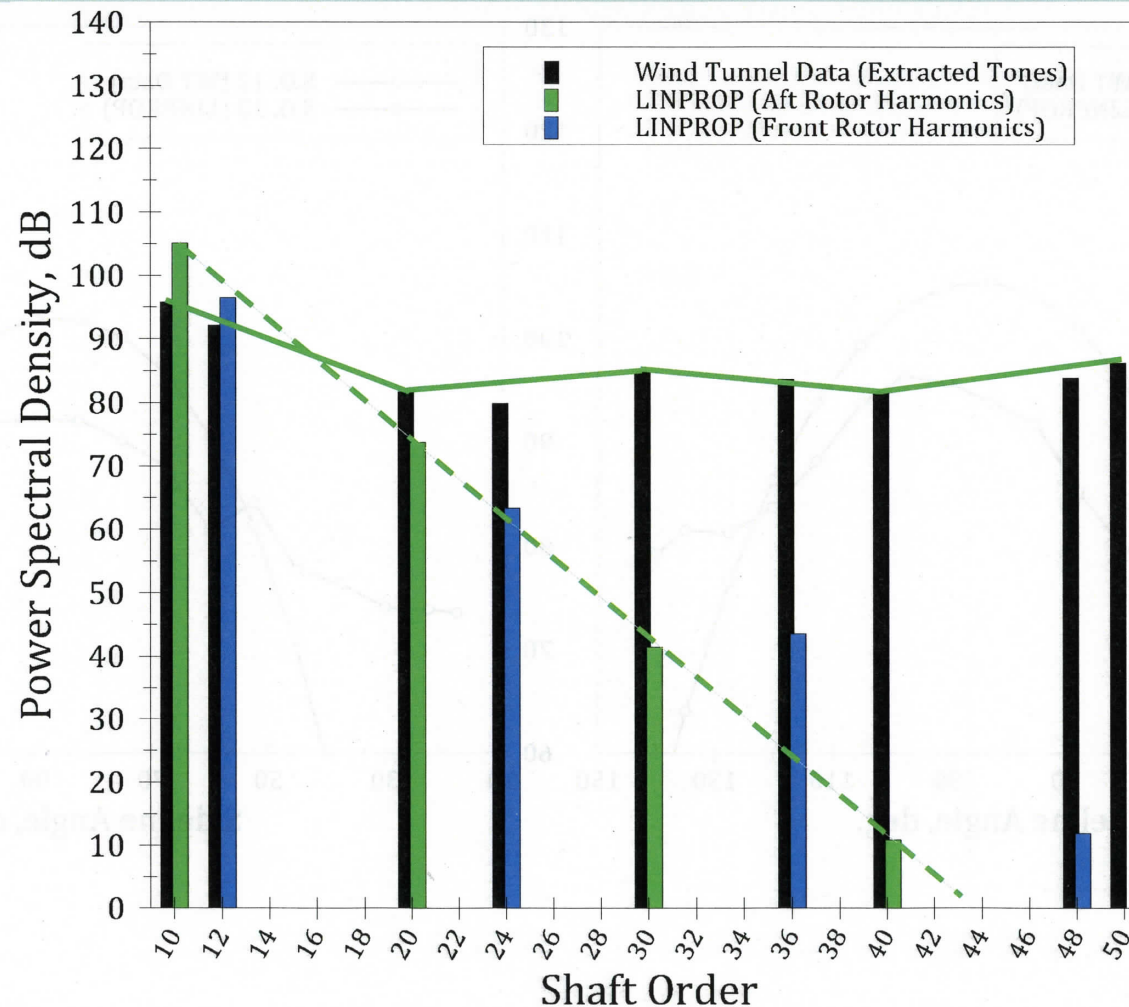
Primary rotor blade passing tones & interaction tones are fairly well predicted.



# Data-Theory Comparisons (Cont'd)



Individual rotor harmonic tones are not well predicted. Likely culprit is the non-linear propagation effect that steepens the primary tone waveform thus distributing additional energy into the higher harmonics

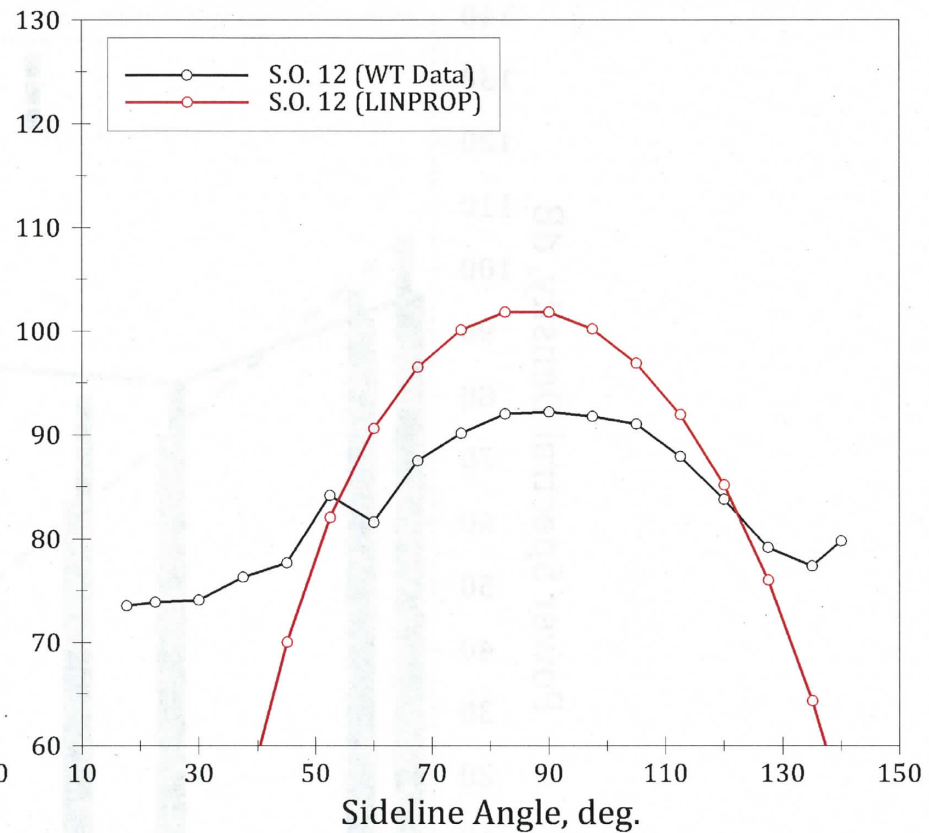
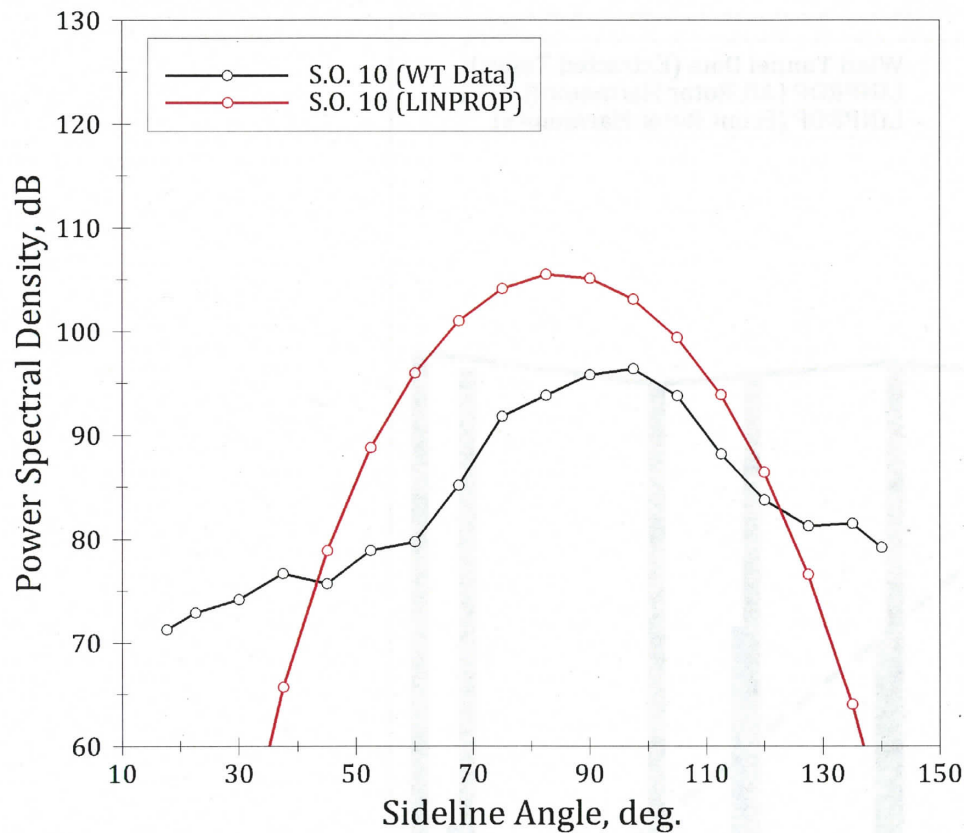




# Data-Theory Comparisons (Cont'd)



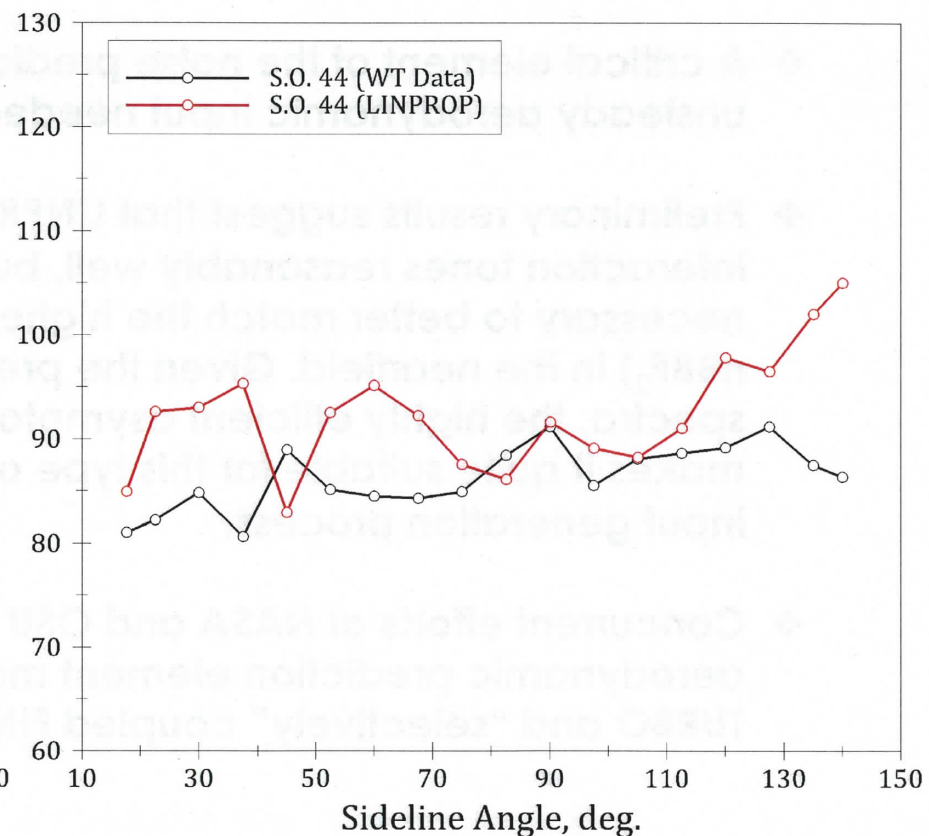
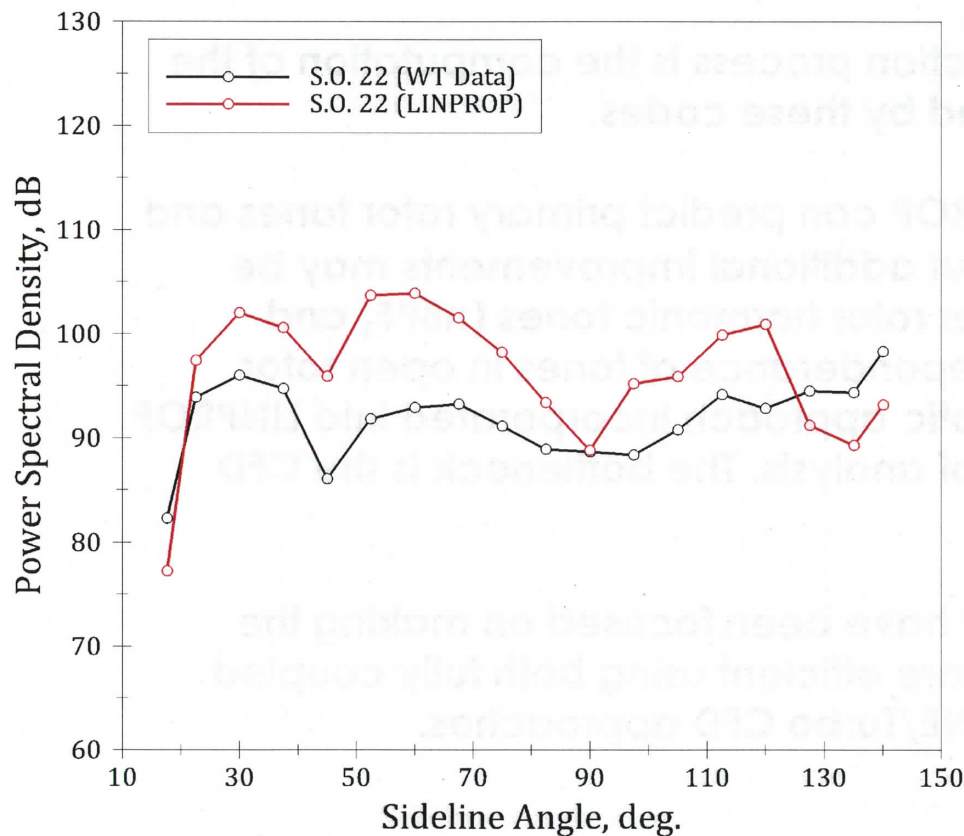
Ex.: Directivity of the primary tones of the two rotors.



# Data-Theory Comparisons (Cont'd)



**Ex.: Directivity of the two principal interaction tones.**





# Summary

---



- ❖ An effort has been underway at NASA to assess and improve NASA open rotor noise prediction tools. LINPROP is one of the NASA codes for open rotor source noise prediction that is being assessed.
- ❖ A critical element of the noise prediction process is the computation of the unsteady aerodynamic input needed by these codes.
- ❖ Preliminary results suggest that LINPROP can predict primary rotor tones and interaction tones reasonably well, but additional improvements may be necessary to better match the higher rotor harmonic tones ( $nBPF_1$  and  $nBBF_2$ ) in the nearfield. Given the preponderance of tones in open rotor spectra, the highly efficient asymptotic approach incorporated into LINPROP makes it quite suitable for this type of analysis. The bottleneck is the CFD input generation process.
- ❖ Concurrent efforts at NASA and OSU have been focused on making the aerodynamic prediction element more efficient using both fully coupled TURBO and “selectively” coupled FINE/Turbo CFD approaches.



---

# Questions?